Geophys. J. Int. (2000) **141,** 204–212

The reduction of aliasing in gravity anomalies and geoid heights using digital terrain data

W. E. Featherstone and J. F. Kirby

School of Spatial Sciences, Curtin University of Technology, GPO Box U1987, *Perth WA* 6845, *Australia. E-mail: tfeather@cc.curtin.edu.au; jfk@vesta.curtin.edu.au*

Accepted 1999 November 23. Received 1999 July 16; in original form 1997 December 30

SUMMARY

Observations of gravity can be aliased by virtue of the logistics involved in collecting these data in the field. For instance, gravity measurements are often made in more accessible lowland areas where there are roads and tracks, thus omitting areas of higher relief in between. The gravimetric determination of the geoid requires mean terrain-corrected free-air anomalies; however, anomalies based only on the observations in lowland regions are not necessarily representative of the true mean value over the topography. A five-stage approach is taken that uses a digital elevation model, which provides a more accurate representation of the topography than the gravity observation elevations, to reduce the unrepresentative sampling in the gravity observations. When using this approach with the Australian digital elevation model, the terrain-corrected free-air anomalies generated from the Australian gravity data base change by between 77.075 and -84.335 mgal (-0.193 mgal mean and 2.687 mgal standard deviation). Subsequent gravimetric geoid computations are used to illustrate the effect of aliasing in the Australian gravity data upon the geoid. The difference between 'aliased' and 'non-aliased' gravimetric geoid solutions varies by between 0.732 and -1.816 m (-0.058 m mean and 0.122 m standard deviation). Based on these conceptual arguments and numerical results, it is recommended that supplementary digital elevation information be included during the estimation of mean gravity anomalies prior to the computation of a gravimetric geoid model.

Key words: aliasing, Australia, digital terrain models, geoid, gravity.

1 INTRODUCTION

When making gravity measurements on land, it is often more convenient to conduct them in areas that are easily accessible by vehicle, such as along tracks and roads for ground-based vehicles. This is because it is inconvenient to carry the instrumentation to locations that would give a more representative coverage of the gravity field. Moreover, the gravimeter's drift dictates that a greater number of observations can be collected during a survey loop if the observation locations, and base-station, are accessible. Another restriction to regular data coverage is denied access due to land ownership and local environmental conditions.

These field practices also apply to geodetic levelling, where it is more convenient to establish benchmarks along accessible tracks and roads. As any computed gravity anomaly is sensitive to elevation uncertainties, gravity measurements are logically made at existing benchmarks that possess a well-defined height. This approach to gravity data acquisition also causes the computed gravity anomalies to be unrepresentative, because the gravity signal in the area, or rather the topographic effect on the gravity anomaly, has not been properly sampled. For instance, if gravity measurements are made in lowland areas where there are benchmarks and accessible roads and tracks, these observations do not sample the gravity signal from areas with higher elevation.

The effect of the irregular sampling geometry in gravimetry is akin to the phenomenon of aliasing in signal processing. Both involve sampling a continuous function at an interval that cannot duplicate that function. In signal processing, the samples are usually made at regular intervals, where information at frequencies higher than twice the sampling frequency is incorrectly represented. According to sampling theory, this high-frequency information becomes *aliased* into the lower frequencies, thus contaminating the sampled function. With gravity data acquisition, the sampling interval is usually irregular, but the consequence is similar: the gravity signal (and its topographic contribution) is sampled such that higher-frequency information is omitted and, as will be shown, aliased into the lower frequencies.

It is likely that this effect is not so important in geophysical gravity data processing, where the aim of the Bouguer reduction is to remove the gravitational signal of the topography. The biased sampling geometry of gravity measurements is arguably an advantage for this application, because the correlation of gravity acceleration with topographic height is reduced *a priori* as a direct consequence of measuring at lower elevations. Uncertainties in the free-air and Bouguer gravity reductions are reduced, because the approximations of the vertical gravity gradient and topographic density apply over a smaller elevation.

In gravimetric geoid determination, however, gravity anomalies are required on the geoid boundary, and these can be approximated from surface observations using the terrain-corrected free-air anomaly. This type of gravity anomaly preserves the mass of the Earth, is harmonic at the geoid, and thus allows Stokes's solution of the geodetic boundary value problem. Evidently, a terrain-corrected free-air anomaly (hereafter referred to as a TCFA anomaly) is highly susceptible to gravity observations that have not correctly sampled the gravitational effect of the topography.

As regional gravity observations have generally been made for geophysical rather than geodetic purposes, the majority of available gravity data is unrepresentative in that the mean TCFA anomaly, computed from only the observations, is not representative of the integral mean TCFA anomaly over the topography. As mentioned, such biased gravity anomalies are often acceptable for geophysical interpretation, where the gravitational effect of topography has been removed, but they are not when determining the geoid. The TCFA anomalies are highly correlated with topography, and are thus highly sensitive to the omission of high-frequency information or aliasing that is introduced by the data acquisition procedure. Therefore, it is necessary to attempt to increase the high-frequency content of the gravity field and reduce the amount of aliasing caused by the unrepresentative observation coverage.

This paper presents the thesis that, prior to a gravimetric determination of the geoid, supplementary information contained within a digital elevation model (DEM) should be used to produce mean TCFA anomalies that are more accurate than mean TCFA anomalies computed from only the gravity observations. This approach is permitted because DEMs are generally less affected by unrepresentative sampling, since they specifically aim to model the form of the topography. In addition, the incorporation of a DEM that is of higher resolution than the gravity observations will yield an increase in resolution in the resulting gravity anomaly grid, which is considered to be a further benefit of the presented technique. Essentially, the DEM provides more accurate mean TCFA anomalies by using high-frequency and representative terrain information to reduce the aliasing often inherent to the gravity observations.

2 MATHEMATICAL REDUCTION OF ALIASING IN GRAVITY ANOMALIES

The principal premise of the reduction of aliasing in gravity anomalies computed from terrestrial gravity measurements on land is based on a reconstruction technique. Supplementary height information from a DEM is used to generate free-air gravity anomalies at unobserved locations on the topography. As a result of the additional topographic information generally contained within a DEM, the reconstructed gravity anomaly field is more representative of the true integral mean over the topography. A mean gravity anomaly is required for the determination of the geoid when Stokes's integral formula is evaluated numerically using quadrature or spectral techniques.

The TCFA anomaly reconstruction technique is described in the following five stages.

2.1 Stage 1

Compute the simple Bouguer anomaly at each of the gravity observation locations according to

$$\Delta g_{\mathrm{B}} = g_{\mathrm{S}} - g(\phi) + \delta g_{\mathrm{F}}(\phi, H) - \delta g_{\mathrm{B}}(H), \tag{1}$$

where g_{S} is the gravity acceleration observed on the Earth's surface; γ is normal gravity at the reference ellipsoid, computed from the geocentric geodetic latitude (ϕ) of the observation using the Somigliana formula (Moritz 1980a); $\delta g_{\mathrm{F}}(\phi, H)$ is the second-order free-air gravity reduction (e.g. Featherstone 1995); and $\delta g_{\mathrm{B}}(H)$ is the Bouguer plate reduction, often based on a constant topographic mass density of 2670 kg m^{-3}. The latter two gravity reductions are functions of H, the elevation of the gravity observation above the geoid, illustrating the importance of having a representative and accurate knowledge of the observation height.

It is argued that the gravimetric terrain correction should not be applied point-by-point to generate the complete Bouguer anomaly at this stage; instead, it will be applied later during the computation of mean TCFA anomalies. Indeed, the application of the gravimetric terrain correction to only the gravity observations will also be aliased, since it is applied to each discrete observation and thus is not representative of the true integral mean over the topography. This is illustrated further by considering the following scenario.

A geographical compartment of arbitrary dimensions contains a single gravity observation made in a valley that is surrounded by higher and rugged terrain. This is considered a realistic example for the reasons outlined in the Introduction. If the terrain correction is applied to this single observation before the computation of the mean gravity anomaly, it will omit the terrain correction that should be applied to every other point over the topography in the compartment. Instead, the terrain correction should be calculated for all DEM cells in the compartment under consideration so that it provides more gravimetric information than would be gained if only the single gravity observation were considered. When averaged, this gives a closer approximation of the true integral mean terrain correction over the topography in the compartment.

The same argument holds for the computation of the atmospheric correction to the gravity anomaly (Ecker & Mittermayer 1969). An atmospheric correction is required to account for the inconsistency between the terrestrial gravity measurements and normal gravity computed from the GRS80 reference ellipsoid (Moritz 1980a). This is necessary because the normal gravity field generated by GRS80 contains a gravitational component due to the mass of the atmosphere, whereas surface observations do not and are affected by an atmospheric gravitational attraction in the opposite direction. An empirical formula for the atmospheric correction is given in, for example, Featherstone *et al.* (1997).

2.2 Stage 2

The simple Bouguer gravity anomaly field is widely regarded as a smooth surface, and is thus particularly suited to interpolation and prediction. Therefore, the computed simple Bouguer anomalies are interpolated onto the grid nodes that define the DEM, which will be denoted by $\Delta g_{\mathrm{B}}^{\mathrm{int}}$. It is acknowledged that the inclusion of the terrain correction will make the Bouguer anomaly an even smoother surface, but the simple Bouguer anomaly is used so as to allow for the addition of the mean terrain correction to yield the mean TCFA.

2.3 Stage 3

Given the interpolated simple Bouguer anomaly at each DEM cell location ($\Delta g_{\mathrm{B}}^{\mathrm{int}}$), reconstruct the free-air anomaly at each point of the grid using the cell height defined by the DEM (H_{DEM}). The reconstruction is achieved simply by applying a negative Bouguer plate reduction, generated for the height of the DEM in each cell, and using the same topographic mass density as in Stage 1. This process essentially restores what the Bouguer plate correction would have removed had gravity data been collected in this element. This yields a *reconstructed* free-air anomaly for each DEM cell within the compartment. The procedure is described mathematically by

$$\Delta g_{\mathrm{F}}(H_{\mathrm{DEM}}) = \Delta g_{\mathrm{B}}^{\mathrm{int}} + \delta g_{\mathrm{B}}(H_{\mathrm{DEM}}), \tag{2}$$

where $\Delta g_{\mathrm{B}}^{\mathrm{int}}$ is the interpolated simple Bouguer anomaly from Stage 2, and $\delta g_{\mathrm{B}}(H_{\mathrm{DEM}})$ is the Bouguer plate correction applied (negatively) for the height of the DEM cell.

The increase in the number of free-air anomaly values is clearly equal to the number of DEM grid cells in the compartment under consideration. Moreover, the approach gives gravity anomalies on a grid, a format that is required for most spectral and quadrature solutions of Stokes's integral.

2.4 Stage 4

The reconstructed free-air anomalies from Stage 3, $\Delta g_{\mathrm{F}}(H_{\mathrm{DEM}})$, are still not ready for a geoid computation, as they do not contain information about the gravity field of the surrounding topography. While the original gravity observations were generally made at locations of lower elevation, this does not necessarily imply a low terrain correction. Therefore, the reconstructed free-air anomalies must be terrain-corrected.

Assuming that the terrain effect is computed from the same DEM as the reconstructed anomaly, as is customary in geoid computations (e.g. Schwarz *et al.* 1990), it can be applied to each reconstructed free-air anomaly without interpolation. Hence, the reconstructed terrain-corrected free-air (TCFA) anomaly is calculated from

$$\Delta g_{\mathrm{TCFA}}(H_{\mathrm{DEM}}) = \Delta g_{\mathrm{F}}(H_{\mathrm{DEM}}) + \delta g_{\mathrm{TC}}(H_{\mathrm{DEM}}), \tag{3}$$

where $\Delta g_{\mathrm{F}}(H_{\mathrm{DEM}})$ is the reconstructed free-air anomaly, and $\delta g_{\mathrm{TC}}(H_{\mathrm{DEM}})$ is the gravimetric terrain correction calculated at each DEM cell.

2.5 Stage 5

Naturally, the estimates of the reconstructed TCFA anomalies are highly susceptible to the quality of the DEM, and any errors present in the DEM will propagate into the reconstructed gravity grid. However, as stated earlier, the construction of a DEM is less susceptible to aliasing by virtue of the topographic data collection scheme. Nevertheless, the grid of reconstructed TCFA anomalies can be averaged to form a coarser grid, which is required for two reasons.

(1) To reduce the magnitude of any errors introduced by the DEM. The DEM heights are usually observed indirectly, commonly by photogrammetric and gridding techniques. The reconstructed gravity anomaly may be subject to an error greater than that of the gravity anomaly computed from the observation itself. The reduction in error by arithmetic averaging is achieved through the general law of propagation of variances, where the error in a mean value of any quantities is less than the errors in the discrete values used to compute that mean value (assuming random errors).

(2) Stokes's integral operator acts as a filter that enhances the contribution of the low-frequency TCFA anomalies to the geoid, whilst at the same time diminishing that of the very high frequencies. As the inclusion of the DEM also introduces a high-frequency signal, most of any error in this frequency band is reduced during the Stokes integration process. As such, it is only necessary to use a lower resolution grid of TCFA anomalies in the computation of the geoid.

Therefore, the reconstructed TCFA anomalies in each cell are averaged into a coarser geographical grid to provide a close as possible representation of the mean anomaly for that compartment. The integral mean gravity anomaly is defined as

$$\overline{\Delta g} = \frac{1}{A} \int\int_{A} \Delta g \, dA, \tag{4}$$

where A is the area of the compartment over which the mean gravity anomaly is required. In practice, this is approximated and computed by

$$\overline{\Delta g} \approx \frac{1}{n} \sum_{i=1}^{n} \Delta g, \tag{5}$$

where n is the number of DEM cells within the compartment. The mean estimates of the TCFA anomaly in eq. (5) can then be used to compute the geoid.

2.6 A conceptual example

To give an initial estimate of the change that can be expected in the mean TCFA anomaly, the following simple, but representative, hypothetical example is used. Consider a geographical compartment with dimensions of $5' \times 5'$, which is bisected by a valley along which one gravity measurement has been made at an elevation of 100 m; this measurement coincides with the geographical centre of the compartment. The free-air anomaly for this station is assumed to be 30.86 mgal, and the corresponding simple Bouguer anomaly is computed as 19.67 mgal when using a mean topographic density of 2670 kg m^{-3}.

In the compartment, the height of this road is $\approx$100 m, and the surrounding mountains reach a height of $\approx$300 m. A DEM of one arc-minute resolution is also available, from which gravimetric terrain corrections have been computed (including elevation information from cells outside this compartment; see, for example, Moritz 1968). Fig. 1 provides a schematic diagram of the grid of DEM heights and the corresponding gravimetric terrain correction for each cell in the compartment. The mean

100 (0.50)	150 (0.60)	200 (0.70)	250 (0.80)	300 (0.90)
150 (0.60)	100 (0.50)	150 (0.60)	200 (0.70)	250 (0.80)
200 (0.70)	150 (0.60)	100 (0.50)	150 (0.60)	200 (0.70)
250 (0.80)	200 (0.70)	150 (0.60)	100 (0.50)	150 (0.60)
300 (0.90)	250 (0.80)	200 (0.70)	150 (0.60)	100 (0.50)

Figure 1. A schematic diagram of a 5′ by 5′ geographical compartment containing one gravity observation ($\Delta g_B = 19.67$ mgal, $\Delta g_F = 30.86$ mgal) situated at the geographical centre of the compartment and in a valley. The 1′ DEM heights (in metres) are given together with the terrain correction (in mgal), which is shown in parentheses for each DEM cell.

30.86 (31.36)	36.46 (37.06)	42.05 (42.75)	47.65 (48.45)	53.24 (54.14)
36.46 (37.06)	30.86 (31.36)	36.46 (37.06)	42.05 (42.75)	47.65 (48.45)
42.05 (42.75)	36.46 (37.06)	30.86 (31.36)	36.46 (37.06)	42.05 (42.75)
47.65 (48.45)	42.05 (42.75)	36.46 (37.06)	30.86 (31.36)	36.46 (37.06)
53.24 (54.14)	47.65 (48.45)	42.05 (42.75)	36.46 (37.06)	30.86 (31.36)

Figure 2. A schematic diagram of the 5′ by 5′ compartment containing the 25 reconstructed free-air and terrain-corrected free-air (in parentheses) anomalies (units in mgal).

terrain correction is 0.66 mgal. The atmospheric gravitational corrections will be neglected in this example, but their effect can be conceptualized and treated in the same way as the gravimetric terrain correction.

Recall that, in gravimetric geoid determination, a mean value of the TCFA anomaly is often required. This quantity will be computed in two ways to illustrate the effect of unrepresentative sampling of the gravity anomalies on the computed geoid.

(1) The (aliased) mean value of the TCFA anomaly is given by the sum of the point free-air anomaly at the geographical centre of the compartment and the gravimetric terrain correction at this point. In this example, the estimate of the mean TCFA anomaly for the compartment is 31.36 mgal (30.86 + 0.50 mgal).

(2) The (non-aliased) mean value of the TCFA is given by the mean of the sum of the reconstructed free-air anomalies and terrain corrections for every cell in the compartment. According to the scheme described above, the simple Bouguer anomaly is assumed to be smooth and interpolates as a constant value over the compartment in this example, thus having a value of 19.67 mgal in each DEM cell. The height of each DEM cell (Fig. 1) is then used with the negative Bouguer plate reduction (eq. 2) to reconstruct a value of the free-air anomaly for each cell. The terrain correction for each cell is then added to each reconstructed free-air anomaly to yield the TCFA anomaly (eq. 3). Fig. 2 shows the reconstructed free-air anomaly in each constituent cell, with the reconstructed TCFA anomaly in parentheses. These values are then averaged over the 25 cells in the compartment (eq. 5) to yield the mean TCFA anomaly.

From the values in Fig. 2, the (non-aliased) mean value of the free-air anomaly over the whole compartment is 39.81 mgal, and the mean (non-aliased) TCFA anomaly is 40.47 mgal. From this simplistic, but reasonably realistic, example it is evident that the compartmental mean TCFA anomaly was underestimated by 9.11 mgal (40.47–31.36 mgal) when using a single (unrepresentative) gravity measurement to estimate the compartmental mean. The converse is true in the case when a gravity observation is made on top of a mountain, where the first method yields a value that is aliased to be an overestimate of the true mean. Given the worst-case scenario of the TCFA anomalies being underestimated in this way over a large area, their effect on the geoid will be systematic. Assuming that a 0.1 mgal systematic gravity anomaly error affects the geoid by ≈ 0.01 m (Vanicek & Martinec 1994), the aliasing in this example can cause an error of ≈ 0.9 m in the geoid. A comparison of the mean values given in Tables 1 and 2 corroborates this crude estimate of the effect on the computed geoid.

This reconstruction technique can also be applied to the generation of mean complete Bouguer anomalies for a subsequent geophysical interpretation. To illustrate the effect in this case, the mean complete Bouguer anomaly over the compartment is estimated in two ways.

(1) The (aliased) mean value of the complete Bouguer anomaly is given by the sum of the point Bouguer anomaly at the station and the gravimetric terrain correction at this point. In the above example, the estimate of the mean complete Bouguer anomaly for the compartment is 20.17 mgal (19.67 + 0.50 mgal).

(2) Assuming that the Bouguer anomaly is smooth, its value at the station applies to the whole compartment. Thus, finding a mean value of the complete Bouguer anomaly over the compartment entails taking the mean of the terrain correction over the cells (Fig. 2) and adding this to the simple Bouguer anomaly. This gives a value of 20.33 mgal (19.67 + 0.66 mgal) for the (non-aliased) mean. Therefore, the mean complete Bouguer anomaly in case 1 above has been underestimated by 0.16 mgal.

The relatively small change in the mean complete Bouguer anomaly in this example is because the terrain corrections are small, and the Bouguer plate reduction has removed most of the correlation of gravitational attraction with topography, and thus reduced the amount of aliasing. However, in areas of particularly rugged topography where the terrain correction can be large, the consideration of the compartmental mean terrain correction becomes more significant in the computation of mean complete Bouguer anomalies.

3 THE EFFECT OF ALIASING ON MEAN GRAVITY ANOMALIES IN AUSTRALIA

As this contribution is concerned with the gravimetric determination of the geoid, and the effect of aliasing is more

significant on the estimation of the mean TCFA than the mean Bouguer anomaly, computations have been performed with TCFA anomalies. Nevertheless, the arguments apply equally to other types of gravity anomaly. The following data sets have been used to determine the mean TCFA anomalies for the Australian continent according to the five stages outlined in Sections 2.1 to 2.5.

A total of 523 497 terrestrial gravity observations were supplied by the Australian Geological Survey Organization (AGSO) as part of its 1992 data release. These data have been cross-checked for gross and detectable systematic errors (Featherstone *et al.* 1997), and all gravity anomalies have been recomputed with respect to the GRS80 reference ellipsoid (Moritz 1980a) and a second-order free-air correction (Featherstone 1995). The latter also accounts for the variation of the vertical normal gravity gradient with latitude. The geodetic coordinates of the gravity observations have also been transformed from the Australian Geodetic Datum to a geocentric reference frame using the procedures described in Featherstone (1995).

The Australian gravity observations were made predominantly at a spacing of ≈ 11 km, with a higher spatial resolution along roads and tracks and in areas where geophysical resource prospecting has been conducted. Most of the data were acquired in the 1960s using helicopter transport and aneroid barometers to determine the elevation of the gravity points. Also, most of the Australian gravity observations were collected before the establishment of the Australian Height Datum (Roelse *et al.* 1971), and are thus not colocated with benchmarks, as is the case in some other countries. Barlow (1977) estimates the observation errors of the Australian gravity data to be ± 0.3 mgal, and the error in their elevation to be ± 4–6 m. These estimates infer an error (assuming independence of the gravity observation, free-air and Bouguer reductions, and no error in the topographic density) in the simple Bouguer anomaly of between 1.35 and 1.99 mgal.

It is worth noting that helicopter-based gravity observations are also subject to aliasing because of the need to have relatively flat areas on which to land the helicopter. In areas of rugged topography, the helicopter usually lands in the sheltered and flat valley regions. In semi-arid regions, where there is gently undulating topography, the helicopter usually lands on elevated areas. This approach to data acquisition causes aliasing of the gravity observations in both areas, with the TCFA anomalies generally underestimated in the highland regions and generally overestimated in semi-arid regions. This effect will be shown later.

The Australian Surveying and Land Information Group (AUSLIG), AGSO and the Department of National Heritage (Carrol & Morse 1996) released the DEM used in this investigation. This DEM was created mostly from AUSLIG spot heights, manually digitized from national topographic maps so as to represent significant topographic features and gradients; the spot heights were sampled at a higher spatial resolution in areas where steep topographic gradients exist. These data form the majority of the information contained within the DEM, but were supplemented with the AGSO gravity observation elevations, radar altimeter profiles, surface drainage and other data. The spatial resolution of this DEM is $9'' \times 9''$, and the estimated precision of the mean height in each cell is 7.5 m (Carrol & Morse 1996)

Ignoring the error in the interpolation routine, and assuming that the DEM and the gravity station elevations are uncorrelated, the corresponding error in the reconstructed free-air anomaly is between 1.59 and 2.16 mgal. This estimate was computed by augmenting the error estimate for the point simple Bouguer anomaly by the error in the reconstruction term, as inferred by the DEM height uncertainty. Clearly, the use of the DEM slightly increases the amount of noise present in the gravity anomalies (1.59–2.16 mgal versus 1.35–1.99 mgal). However, these estimates only apply to the reconstructed and calculated gravity anomalies at each DEM cell, respectively. When these values are averaged, the general law of propagation of variances dictates that the (random) error in the mean gravity anomaly is reduced.

To illustrate the above, consider the example of a $6' \times 6'$ compartment containing reconstructed free-air anomalies on a $9'' \times 9''$ grid. This compartment comprises 1600 DEM cells, each with an individual error of 1.59–2.16 mgal, thus giving an error of 0.04–0.05 mgal in the mean anomaly. Conversely, the error of the AGSO gravity anomaly, assuming a single observation per compartment (which holds over most of the continent for this grid spacing), remains at between 1.35 and 1.99 mgal. Note, however, that the above error estimates ignore the error committed by the gridding algorithm and assume independence of some quantities that are probably correlated.

In order to quantify the extent of aliasing on the TCFA anomalies, two grids of gravity anomalies were generated over the Australian continent as follows. In both instances, the terrain corrections were taken from a $27''$ grid generated from the DEM by Kirby & Featherstone (1999). This coarser grid was required in order to avoid the numerical instability in Moritz's (1968) algorithm for dense DEM grids (*cf.* Martinec *et al.* 1996).

(1) The AGSO free-air anomalies were augmented by interpolated gravimetric terrain corrections at each observation point, then arithmetically averaged to form a $6' \times 6'$ grid of mean TCFA anomalies. The grid spacing of ≈ 11 km corresponds to the mode of the spacing of the Australian gravity observations. This grid will be termed the aliased gravity grid (AGG).

(2) The second gravity grid was generated using the five-stage reconstruction approach (Sections 2.1 to 2.5). The simple Bouguer anomalies (eq. 1) were interpolated onto a $9'' \times 9''$ grid, which is commensurate with the Australian DEM. Free-air anomalies were then reconstructed from this grid of simple Bouguer anomalies using the mean height of each DEM cell (eq. 2). The reconstructed free-air anomalies and gravimetric terrain corrections were then averaged (eq. 5) onto a $6' \times 6'$ grid. This will be termed the non-aliased gravity grid (NAGG).

The interpolation of the simple Bouguer anomalies, computed from the discrete gravity observations, used the tensioned spline algorithm of Smith & Wessel (1990). Whilst the use of least-squares collocation (Moritz 1980b) is widespread for gravity gridding in physical geodesy, the tensioned spline algorithm was used here as it is also suited to potential field data.

Fig. 3 shows the difference between the mean TCFA anomalies based on the AGG and those based on the more representative NAGG, which is based on the reconstructed free-air anomalies with the mean terrain correction applied over each compartment. Fig. 3 indicates that the difference between the AGG and NAGG fields contains short-wavelength features, which

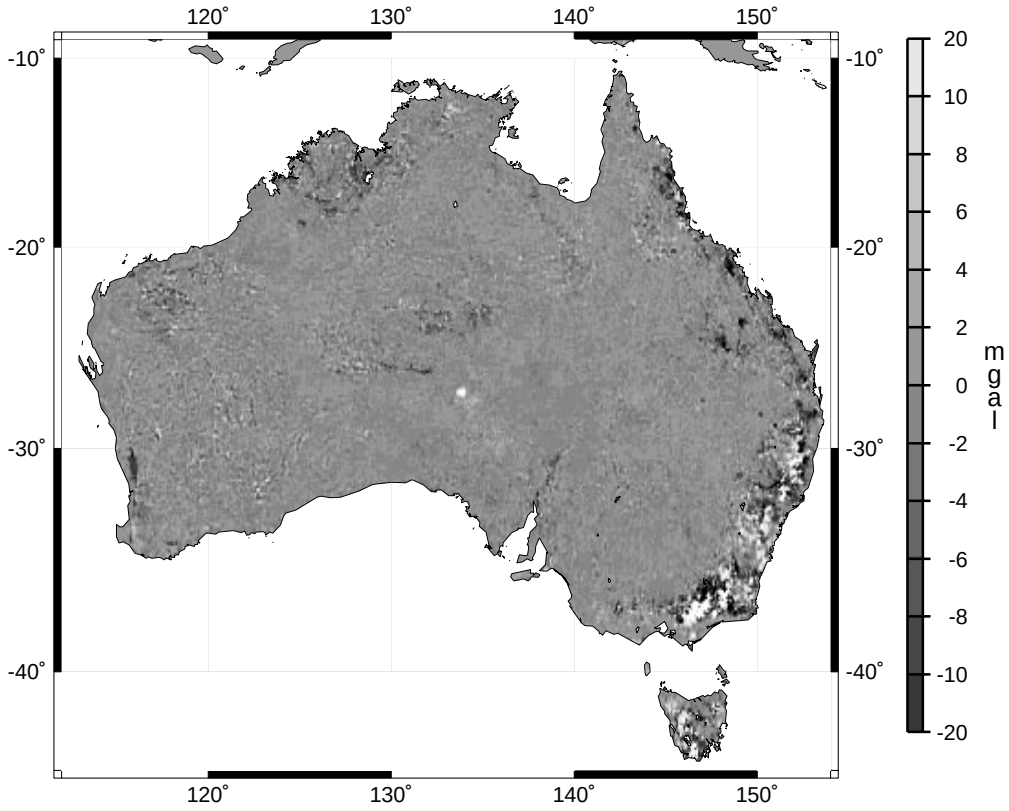

Figure 3. The differences between mean TCFA anomalies computed from point gravity observations and mean TCFA anomalies computed from the five-stage reconstruction technique described in Sections 2.1 to 2.5 (units in mgal).

are highly correlated with the mountainous regions of the Great Dividing Range in eastern Australia and in Tasmania. This is expected because of the increase in resolution provided by the reconstruction method. However, the high-frequency detail in Fig. 3 obscures any evidence of aliasing (a leakage of short wavelengths into the long wavelengths). Therefore, the difference between the AGG and NAGG fields in Fig. 3 is low-pass filtered to make any aliasing more apparent. A 400-km low-pass cosine filter was applied to the gravity differences in Fig. 3, which gives the low-frequency component of this gravity difference, shown in Fig. 4. It is concluded from Fig. 4 that the long-wavelength differences between the AGG and NAGG fields arise from an aliasing effect.

In Fig. 4, the low-frequency component of the difference between the AGG and NAGG fields is generally negative throughout the more mountainous regions of Australia. These include the Great Dividing Ranges of eastern Australia, the McDonnell Ranges (centred at 25°S, 133°E), the Pilbara (centred at 16°S, 128°E) and the Hamersley Ranges (centred at 22°S, 118°E). This indicates that the mean TCFA anomalies computed from only the gravity observations are underestimates of the integral-mean TCFA anomalies in each compartment. This is because the majority of terrestrial gravity observations that have been made in these regions are in the accessible lower-lying areas, and the anomalies computed from only the observations use an underestimate of the true mean height in each compartment. The aliasing effect also manifests itself in areas where the TCFA anomalies computed from only the observations are overestimates of their integral-mean values, such as in the Nullarbor Plain (centred at 31°S, 129°E). As mentioned earlier, helicopters would generally have landed on raised ground, thus providing an overestimate of the mean height over the region.

Table 1 shows the statistical distribution of the differences between the AGG and NAGG fields. The maximum positive difference of 77.075 mgal occurs in the lowland regions of central Western Australia, where the mean TCFA anomalies computed from only the observations have been overestimated. Similarly, the maximum negative difference of −84.335 mgal occurs in the Great Dividing Ranges, where the mean TCFA anomalies computed from only the observations have been underestimated. The mean difference of −0.193 mgal and Fig. 4 indicate that, over the whole of Australia, the mean TCFA anomalies have generally been underestimated.

4 THE EFFECT OF ALIASING ON GRAVIMETRIC GEOID COMPUTATIONS IN AUSTRALIA

In order to estimate the effects of using the unrepresentative TCFA anomalies on the determination of the geoid, two gravimetric geoid solutions were computed from the AGG and NAGG data sets, and then compared.

Table 1. Statistical summary of the differences between the AGG and NAGG grids over Australia (units in mgal).

	max	min	mean	std dev	rms
difference	77.075	−84.335	−0.193	2.687	2.694.

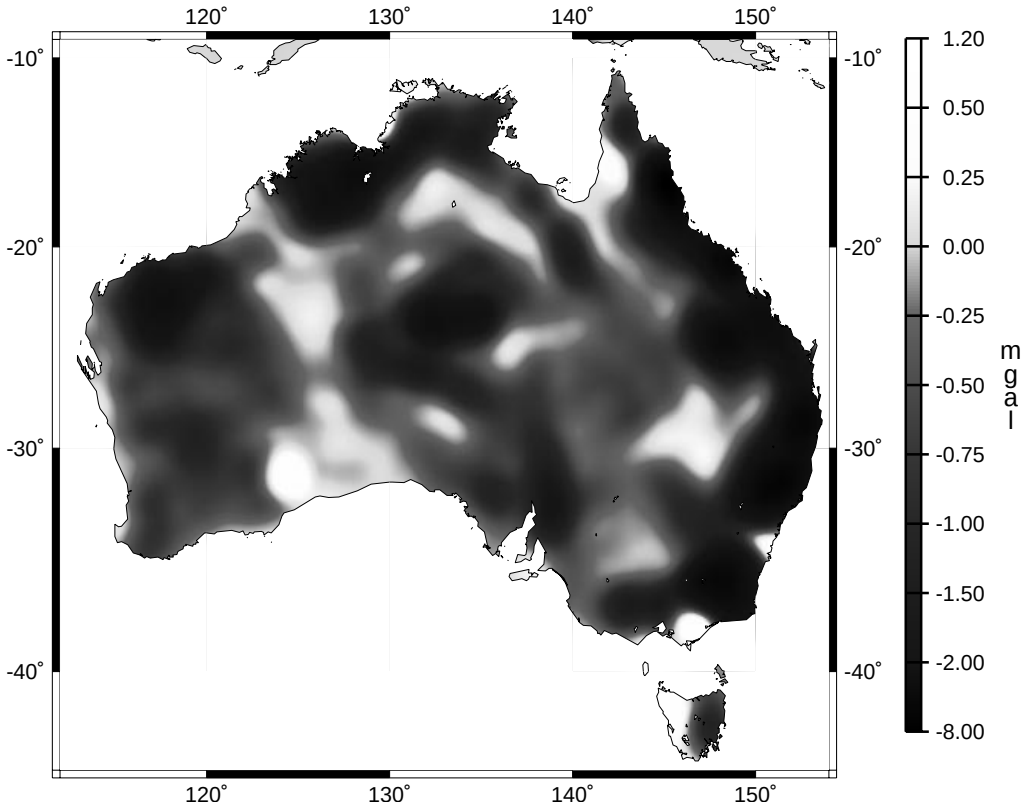

Figure 4. Low-pass filtered version of Fig. 3, using a 400-km low-pass cosine filter, to show the long-wavelength differences due to aliasing in the gravity observations (units in mgal).

As is customary in modern geoid computation, the gravity field implied by a global geopotential model was first removed from the two TCFA anomaly grids (the AGG field and the NAGG field). This yields what are commonly called residual gravity anomalies. The corresponding effect of the global geopotential model on the geoid is subsequently restored after computation, and this method is therefore commonly called the remove-compute-restore technique. The global geopotential model used in this investigation was EGM96 (Lemoine *et al.* 1997), which was computed to its maximum spherical harmonic degree of 360.

The arguments presented in Section 2.1 for the application of the terrain corrections also hold for the computation of residual gravity anomalies from the global geopotential model. Consider the example where a single point gravity observation is used to compute the residual mean gravity anomaly. If the gravity anomaly implied by the global geopotential model is removed from only the point observation, it will not necessarily be representative of the integral mean value over a compartment. Therefore, the mean value should be computed for each compartment. This can be achieved either by computing the gravity anomaly from the global geopotential model for each cell in the compartment, then averaged according to eq. (5), or by using the smoothing factors described by Pellinen (1966) (see also Rapp 1977). In this study, the former approach was used to produce what will be called the residual aliased gravity grid (RAGG) from the AGG field, and the residual non-aliased gravity grid (RNAGG) from the NAGG field.

The computational technique used to compute the corresponding residual geoid undulations from each residual gravity grid was the 1-D fast Fourier transform, or 1D-FFT (Haagmans *et al.* 1993). The 1D-FFT approach to residual gravimetric geoid computation requires a regular grid of residual TCFA anomalies as input. Therefore, the proposed approach of combining point gravity observations with a DEM to produce a regular geographical grid is particularly suited to data preparation for such determinations of the geoid. The 1D-FFT computer software used is a modified version of that kindly supplied by Professor M. G. Sideris of the University of Calgary, Canada.

The two, $6' \times 6'$ grids of residual TCFA anomalies (RAGG and RNAGG) were used in a 1D-FFT determination of the residual TCFA co-geoid, which is referenced to the degree-360 spherical harmonic expansion of EGM96. The spectral geoid determinations used a 2° integration radius, as implemented in the FFT software by Featherstone & Sideris (1998) (see also Forsberg & Featherstone 1998). This integration radius was chosen arbitrarily so as to illustrate the relative effect of the two TCFA anomaly grids on the computed geoid.

In order to compute the geoid height relative to the reference ellipsoid, the geoidal undulations provided by the degree-360 expansion of EGM96 must be added to the residual co-geoid undulations, as must be the indirect effect of the terrain condensation applied to convert the co-geoid to the geoid (e.g. Wichiencharoen 1982). However, as these two calculation stages will be common to each residual geoid solution, it is sufficient to compare only the residual solutions to illustrate the effects of aliasing and unrepresentative sampling in the TCFA anomalies on the geoid. Fig. 5 shows the difference between the residual co-geoids computed from the RAGG and RNAGG fields, and Table 2 shows their statistical distribution.

In Fig. 5, the differences in the two geoid solutions are highly correlated with the differences shown in Fig. 4. This is because

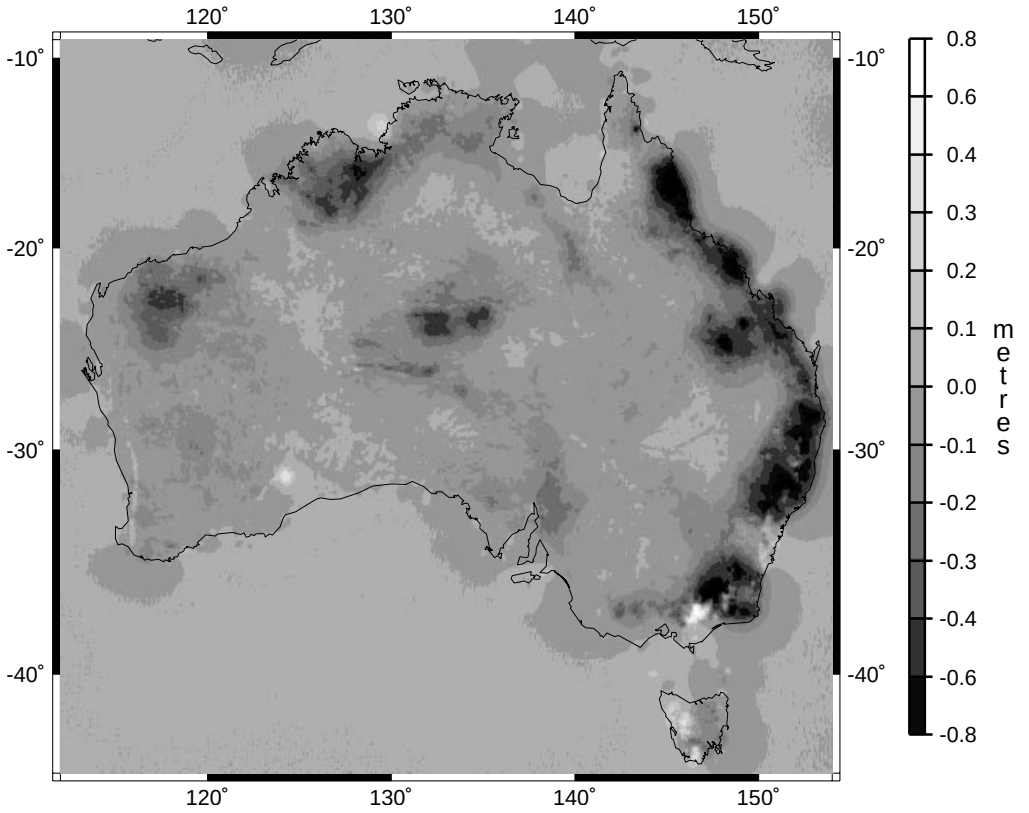

Figure 5. Differences between gravimetric co-geoids computed from the RAGG and RNAGG data sets (units in metres).

Table 2. Statistics of the differences between the two co-geoid solutions for a 6′ by 6′ grid over Australia (units in metres).

	max	min	mean	std dev	rms
difference	0.732	−1.816	−0.058	0.122	0.135

Stokes's kernel function is always positive in the 2° integration radius. Furthermore, the effect of the high-frequency differences between the AGG and NAGG fields (Fig. 3) on the geoid is less because Stokes's convolution is a filtering process whereby the low frequencies are enhanced and high frequencies diminished in the resulting gravimetric geoid. However, the use of the reconstruction technique does add some high-frequency information into the geoid solution (Fig. 5). Note also that the differences between the geoid solutions are seen to extend approximately 2° from the Australian coastline (Fig. 5). This is due to the fact that the gravimetric geoid solution is affected by gravity data in the integration domain of the 2° cap, so the difference between the RAGG and RNAGG data sets extends into and influences the geoid computed in marine regions.

As for the TCFA anomalies (Table 1), the maximum positive difference of 0.732 m occurs in the lowland regions of central Western Australia, where the residual mean TCFA anomalies and hence geoid have been overestimated when using only the observed gravity data. Similarly, the maximum negative difference of −1.816 m occurs in the Great Dividing Ranges, where the mean TCFA anomalies and resulting geoid have been underestimated when using only the observed gravity data.

5 SUMMARY, CONCLUSIONS AND RECOMMENDATIONS

A mathematical reconstruction technique has been proposed whereby digital elevation data are used to reduce the effects of unrepresentative sampling in observations of the Earth's gravity field. Gravity anomalies computed from terrestrial gravity measurements on land are aliased due to the logistics of collecting such data, it being more convenient to collect measurements in accessible areas. Therefore, the mean gravity anomalies (whether free-air, terrain-corrected free-air or Bouguer) computed directly from these measurements are not necessarily representative of the true integral mean over the topography.

The proposed approach uses supplementary high-frequency information by way of a digital elevation model to produce more accurate estimates of the true integral mean of the gravity anomaly over the topography. This approach succeeds because a DEM is specifically constructed to give an accurate representation of the topography, whereas the gravity observation elevations often do not. An additional benefit of using the reconstruction approach is that gravity anomalies may be predicted in areas where no gravity observations have been made.

The implementation of the five-stage reconstruction technique can be summarized as follows. Simple Bouguer anomalies are computed from the gravity observations and then interpolated to the geographical locations of the DEM cells to give a high-resolution grid of these anomalies. The reverse Bouguer plate reduction is then applied to each simple Bouguer anomaly

in this grid using the height of the DEM cell to reconstruct a free-air anomaly. The gravimetric terrain correction is also computed for all the DEM cells in each compartment, and added to each of the reconstructed free-air anomalies. A mean value of the TCFA anomaly is then computed for each compartment. These mean TCFA anomalies are therefore less affected by unrepresentative sampling and more suited for use in the gravimetric determination of the geoid.

Results for Australia on a $6' \times 6'$ grid have been used to illustrate the effect of aliasing on both the computations of mean TCFA anomalies and gravimetric geoid undulations. The difference between gravity anomalies derived from the observed (aliased) and reconstructed (non-aliased) gravity grids show a mean difference of -0.193 mgal in the TCFA anomalies and -0.058 m in the resulting gravimetric geoid. This indicates that the majority of the Australian gravity anomalies, computed from the observed gravity data alone, are unrepresentative of the true gravity field and thus do not allow the estimation of accurate mean anomaly values. Therefore, it is recommended that the proposed reconstruction technique be used to compute more accurate estimates of the mean TCFA anomaly prior to the determination of the geoid from terrestrial gravity data.

ACKNOWLEDGMENTS

We wish to thank the Australian Geological Survey Organization (AGSO) for providing the Australian gravity data-base; the Australian Surveying and Land Information Group (AUSLIG) for providing the digital elevation model; and Professor M. G. Sideris of the University of Calgary for providing a suite of FFT geoid computation software, which has been modified for use in this study. This research was funded as part of Australian Research Council grant A49331318. Thanks are also extended to the three reviewers for their time taken to consider this manuscript.

REFERENCES

Barlow, B.C., 1977. Data limitations on model complexity; 2-D gravity modelling with desk-top calculators, *Bull. Aust. Soc. expl. Geophys.,* **8,** 139–143.

Carrol, D. & Morse, M.P., 1996. A national digital elevation model for resource and environmental management, *Cartography,* **25,** 43–49.

Ecker, E. & Mittermayer, E., 1969. Gravity corrections for the influence of the atmosphere, *Boll. Geof. Teor Appl.,* **11,** 70–80.

Featherstone, W.E., 1995. On the use of Australian geodetic datums in gravity field determination, *Geomatics Res. Aust.,* **61,** 17–36.

Featherstone, W.E. & Sideris, M.G., 1998. Modified kernels in spectral geoid determination: first results from Western Australia, in *Geodesy on the Move: Gravity, Geoids, Geodynamics and Antarctica,* pp. 188–193, eds Forsberg, R., Feissl, M. & Dietrich, M., Springer-Verlag, Berlin.

Featherstone, W.E., Kearsley, A.H.W. & Gilliland, J.R., 1997. Data preparations for a new Australian gravimetric geoid, *Aust. Surv.,* **42,** 33–44.

Forsberg, R. & Featherstone, W.E., 1998. Geoids and cap sizes, in *Geodesy on the Move: Gravity, Geoids, Geodynamics and Antarctica,* pp. 194–200, eds Forsberg, R., Feissl, M. & Dietrich, M., Springer-Verlag, Berlin.

Haagmans, R.R., de Min, E. & van Gelderen, M., 1993. Fast evaluation of convolution integrals on the sphere using 1D-FFT, and a comparison with existing methods for Stokes's integral, *Man. Geod.,* **18,** 227–241.

Kirby, J.F. & Featherstone, W.E., 1999. Terrain correcting the Australian gravity database using the national digital elevation model and the fast Fourier transform, *Aust. J. Earth Sci.,* **46,** 555–562.

Lemoine, F.G. *et al.,* 1997. The development of the NASA, GSFC and DMA joint geopotential model, in *Gravity, Geoid and Marine Geodesy,* pp. 461–469, eds Segawa, J., Fujimoto, H. & Okubo, S., Springer-Verlag, Berlin.

Martinec, Z., Vanicek, P., Mainville, A. & Veronneau, M., 1996. Evaluation of topographical effects in precise geoid computation from densely sampled heights, *J. Geod.,* **70,** 746–754.

Moritz, H., 1968. On the use of the terrain correction in solving Molodensky's problem, *Report 108,* Department of Geodetic Science and Surveying, Ohio State University, Columbus.

Moritz, H., 1980a. Geodetic Reference System 1980, *Bull. Geod.,* **54,** 395–405.

Moritz, H., 1980b. *Advanced Physical Geodesy,* Wichmann-Verlag, Karlsruhe.

Pellinen, L.P., 1966. A method for expanding the gravity potential of the Earth in spherical functions, in *Trans. Central Scientific Res. Inst. Geodesy, Aerial Survey and Cartography, 171,* Nedra, Moscow.

Rapp, R.H., 1977. The relationship between mean anomaly block sizes and spherical harmonic representations, *J. geophys Res.,* **82,** 5360–5364.

Roelse, A., Granger, H.W. & Graham, J.W., 1971. The adjustment of the Australian levelling survey 1970–1971, *Technical Report 12,* Division of National Mapping, Canberra.

Schwarz, K.P., Sideris, M.G. & Forsberg, R., 1990. The use of FFT techniques in physical geodesy, *Geophys. J. Int.,* **100,** 485–514.

Smith, W.H.F. & Wessel, P., 1990. Gridding with continuous curvature splines in tension, *Geophysics,* **55,** 293–305.

Vanicek, P. & Martinec, Z., 1994. The Stokes-Helmert scheme for the evaluation of a precise geoid, *Man. Geod.,* **19,** 119–128.

Wichiencharoen, C., 1982. The indirect effects on the computation of geoid undulations, *Report 336,* Department of Geodetic Science and Surveying, Ohio State University, Columbus.